Pramāṇa, Vol. 10, No. 4, April 1978, pp. 429–446, © printed in India.

Self-similar solutions for implosion and reflection of coalesced shocks in a plasma: Spherical and cylindrical geometries

L K CHAVDA and SUDHANSHU S JHA*
Physics Department, South Gujarat University, Surat 395 007
*Tata Institute of Fundamental Research, Bombay 400 005

MS received 16 December 1977

Abstract. Approximate analytic solutions to the self similar equations of gas dynamics for a plasma, treated as an ideal gas with specific heat ratio $\gamma = 5/3$, are obtained for the implosion and subsequent reflection of various types of shock sequences in spherical and cylindrical geometries. This is based on the lowest-order polynomial approximation, in the reduced fluid velocity, for a suitable nonlinear function of the sound velocity and the fluid velocity. However, the method developed here is powerful enough to be extended analytically to higher order polynomial approximations, to obtain successive approximations to the exact self-similar solutions. Also obtained, for the first time, are exact asymptotic solutions, in analytic form, for the reflected shocks. Criteria are given that may enable one to make a choice between the two geometries for maximising compression or temperature of the gas. These solutions should be useful in the study of inertial confinement of a plasma.

Keywords. Self-similar equations; shock sequences; implosion; asymptotic solution; spherical and cylindrical geometries.

1. Introduction

Recent experimental and theoretical schemes for producing fusionable temperatures using high-power ion beams or relativistic electron beams (Bogolyubskii *et al* 1976; Clauser *et al* 1977; Chang *et al* 1975), and the experiments using lasers for the same purpose under way at many laboratories, including the Lawrence Livermore Laboratory, have given a great impetus to the study of the dynamics of the implosion of shock waves in a thermonuclear plasma. The implosion helps reduce the input energy by compressing the fusion fuel to high densities before it is heated to fusionable temperatures. It also obviates the necessity of external magnetic confinement of the plasma so produced. Classical studies of the implosion problem in an ideal gas, although mostly numerical, produced a number of important results. Among these is the well-known study by Guderley (1942) that the maximum compression in the implosion of a single strong shock is limited to a definite value for any γ, where γ is the ratio of specific heats in the ideal gas. However, these studies involve a great deal of numerical computation, and do not throw much light on the way the various parameters affect the dynamics of the implosion and the subsequent reflection of shock waves. In this paper, we seek approximate but sufficiently accurate analytic solutions to the problem, for both the spherical and cylindrical geometries. Some work along these lines for the spherical geometry has already been reported by us recently (Jha and Chavda 1977). As already shown there, at high temperatures

being considered here, the fusionable material (*D-T* pellet) can be treated as an ideal gas of $\gamma = 5/3$. The analytic approach presented here enables us to study the parameters that control the growth of the pressure, the temperature, etc. much more transparently. In particular, we can exhibit explicitly the role played by the geometry of the implosion. We also present, for the first time, the exact asymptotic solution to the motion of the reflected shocks in an analytic form. The paper is organised as follows. In section 2, we present for an ideal gas, the one-dimensional hydrodynamic partial different equations for an arbitrary geometry. The self-similar equations, which give the exact behaviour at the point of implosion, and their symmetry and non-linearity properties are also discussed in this section. Formal exact solutions to the self-similarity equations are presented in the form of continued fractions in section 3. More useful approximate solutions are presented in section 4, where the exact asymptotic solution to the motion of the reflected shocks is also to be found. We conclude this work in section 5.

2. Self-similarity equations and their symmetry and non-linearity properties

2.1. *Hydrodynamic equations*

Let u, ρ, p, c define the gas velocity in the symmetry direction, the density of the gas, the pressure of the gas and the speed of sound in the gas, respectively. All these quantities are measured at the point of observation at all times. The point of observation is at a distance r from the centre of symmetry. For the spherical geometry $r = 0$ is the centre of the sphere and for the cylindrical geometry $r = 0$ is the axis of the cylinder. In both these cases, u represents the radial velocity. The time $t = 0$ is the time at which the incident shock front arrives at the centre of symmetry. In the absence of dissipation and the external source term, we can then write the hydrodynamic conservation laws for mass, momentum and energy in the form (Stanyukovich 1960)

$$\frac{\partial}{\partial t}(\ln\rho) + u\frac{\partial}{\partial r}(\ln\rho) + \frac{Nu}{r} + \frac{\partial u}{\partial r} = 0 \tag{1}$$

$$\frac{\partial u}{\partial t} + u\frac{\partial u}{\partial r} + \frac{1}{\rho}\frac{\partial p}{\partial r} = 0 \tag{2}$$

$$\frac{\partial}{\partial t}\ln(p\rho^{-\gamma}) + u\frac{\partial}{\partial r}\ln(p\rho^{-\gamma}) = 0 \tag{3}$$

where N equals 0, 1, 2 for the plane, the cylindrical and the spherical geometries, respectively.

2.2. *Self-similar equations*

We consider a spherical or a cylindrical fuel pellet consisting of an equal mixture of deuterium (D) and tritium (T), at solid densities. Relativistic electrons, lasers or ion beams provide the piston action for the implosion. We treat the *D-T* plasma as

an ideal gas with $\gamma = 5/3$ and an average electron-ion mass $M/2$ approximately, where M is the mass of an ion. Although the formalism presented here is valid for arbitrary γ, we shall present final numerical results for the important case of $\gamma = 5/3$ only. In this paper, we examine the following three types of shocks: (a) A single strong shock (the $1S$ case), (b) A coalesced sequence consisting of a single strong shock followed by $m-1$ weak ones (the $1S(m-1)W$ case) launched in such a way that they all merge into a single shock front at a distance r_m from the centre of symmetry, (c) A coalesced sequence of m weak shocks launched as in (b). In each case, after the coalescence of the shocks, one must consider four regions. We denote by A the region in which the incident (coalesced) shock front has not yet reached the point of observation ($t < 0$). Region B is one where this incident shock front has passed the observation point but has not yet reached the centre of symmetry (t still less than zero). C denotes the region where the front is reflected from the centre, but has not yet arrived at the point of observation ($t > 0$), and D is the region where the reflected shock front is past the observation point (t greater than zero).

The characteristic variables of the problem are p, u, ρ, r, t. The fundamental dimensions from which these can be constructed are the length (L), the mass (M) and the time (T). We shall, however, take $R_I(t)$, ρ_0, and $\dot{R}_I(t)$ as the independent dimensional quantities to correspond to L, M, T. Here ρ_0 is the density of the undisturbed gas and $R_I(t)$ is the position of the incident (coalesced) shock front at time t. Also, since $\rho_0 \dot{R}_I^2(t)$ has the dimensions of pressure, we shall take the former as the pressure scale. Using these scales, we may construct corresponding reduced, dimensionless functions from p, u, ρ and c. These reduced functions will, in general, depend upon (See e.g., Zeldovich and Raizer 1967) two dimensionless variables $r/R_I(t)$ and $t/|t_0|$ where $|t_0|$ is the time it takes the incident shock front to reach the centre of symmetry from the point of observation. We note that $t_0 < 0$ because we have taken $t = 0$ to be the time at which the incident shock front arrives at the centre of symmetry. For small negative t, one may expand $R_I(t)$ as

$$R_I(t) = \Sigma_q \alpha_q (-t)^q; \quad t < 0 \ldots \tag{4}$$

For sufficiently small (negative) values of t one may approximate it as

$$R_I(t) \simeq \xi (-t)^\alpha; \quad t < 0 \tag{5}$$

where α is the smallest power in the expansion, eq. (4). Asymptotically, as $t \to 0$, eq. (5) is exact. The region where eq. (5) is approximately valid is the region of self-similarity, and α is the self-similarity index. In this region, in view of eq. (5), the variables $r/R_I(t)$ and $t/|t_0|$ are no longer independent of each other. Consequently the reduced functions constructed from p, u, ρ, c will depend upon only one variable

$$s = t/|t_0| \tag{6}$$

we assume that the point of coalescence, r_m, and the point of observation $r(r < r_m)$ are both approximately inside the region of self-similarity. From eq. (6) it follows that the incident shock front arrives at the point of observaton at $s = -1$. Furthermore,

$$R_I(t_0) = r = \xi(-t_0)^{\alpha}; \quad |t_0| = (r/\xi)^{1/\alpha} \tag{7}$$

$$r/R_I(t) = (-s)^{-\alpha}; \quad s < 0 \tag{8}$$

$$D_I(r) \equiv \dot{R}_I(t_0) = -\alpha\ \xi^{1/\alpha}\ r^{(\alpha-1)/\alpha} \tag{9}$$

$$\dot{R}_I(t) = D_I(r)\,(-s)^{\alpha-1}; \quad s < 0 \tag{10}$$

and

$$r/t = \frac{1}{\alpha s}|D_I(r)| \tag{11}$$

where $D_I(r)$ is the speed of the incident shock front when the latter arrives at the point of observation. It can be shown that the motion after the implosion ($t > 0$) (Guderley 1942; Zeldovich and Raizer 1967) is also self-similar with the same α. Thus, for the position $R_R(t)$ for the reflected front we can write

$$R_R(t) = \xi(t/s^*)^{\alpha}; \quad t > 0 \tag{12}$$

$$\dot{R}_R(t) = D_R(r)\,s^{\alpha-1}; \quad D_R(r) = |D_I(r)|/s^* \tag{13}$$

$$(s/s^*)^{-\alpha} = r/R_R(t); \quad s > 0 \tag{14}$$

where $s = s^*$ corresponds to the return of the reflected shock front to the point of observation. In the region of self-similarity, one can define the reduced dimensionless functions as follows:

$$u = (r/t)\,V(s) \tag{15}$$

$$\rho = \rho_0\,G(s) \tag{16}$$

$$c^2 = (r^2/t^2)\,Z(s). \tag{17}$$

We recall that p, ρ, u, c are measured at the point of observation at all times. In the region B, the gas is moving towards the centre of symmetry. Therefore u is negative but so also is t. Thus, in view of eq. (15), $V(s) > 0$, for $s < 0$. In the region C, reflection of the incident shock front is taking place at the centre of symmetry. However, the reflected shock front has not yet reached the point of observation. Thus, at the point of observation, the gas is still moving towards the centre of symmetry. Consequently u is still negative although $t > 0$. Therefore, in view of eq. (15), $V(s) < 0$, for $s > 0$, but $s < s^*$. Similarly, in the region D, $V(s) > 0$, $s > s^*$. G and Z are, of course, positive in all regions. In terms of the reduced functions, one can show that the three partial differential eqs (1)–(3) reduce to three ordinary differential equations in the region of self-similarity. One can also obtain an exact adiabatic integral from these three ordinary differential equations (Zeldovich and Raizer 1967). The two ordinary differential equations and the adiabatic integral are given by (Jha and Chavda 1977; Stanyukovich 1960).

$$\frac{d\ln Z}{dV} = \frac{\gamma-1}{\alpha-V} - \frac{\alpha[(1+(N+1)\,\gamma-2)V-2]}{\alpha-V}\,\frac{d\ln|s|}{dV} \tag{18}$$

$$-\alpha\frac{d\ln|s|}{dV} = \frac{(\alpha-V)^2-Z}{Z[(N+1)V-\mu]-V(1-V)(\alpha-V)} \equiv \frac{\Delta}{\Delta_1}. \tag{19}$$

$$G = C\,s^{-2\alpha(N+1)\sigma}\,Z^{\alpha(N+1)\,\sigma}\,(\alpha-V)^{2(1-\alpha)\,\sigma};\ C = \text{const}, \tag{20}$$

where

$$\mu = 2(1-\alpha)/\gamma \text{ and } 1/\sigma = \alpha[(N+1)\,\gamma+1\,-N]\,-2. \tag{21}$$

Note that one may also write eq. (18) as

$$\frac{dZ}{dV} = \frac{Z[g_1(V)Z-g_2(V)]}{g_3(V)\,Z-g_4(V)} \tag{22}$$

where g_i are the known polynomials in V:

$$g_1 = 2(1-\alpha)+2\gamma(\alpha-V);\ g_2 = 2\gamma(\alpha-V)^2\,(1-V)+\gamma(\gamma-1)\,V(\alpha-V)\times(2V-3\alpha+1)$$

$$g_3 = 3\gamma\,(\alpha-V)\,[V-2\,(1-\alpha)/3\gamma];\quad g_4 = \gamma(\alpha-V)^2\,(1-V)V$$

2.3. *Symmetry and nonlinearity properties*

Since eq. (22) cannot be exactly solved, we must study its symmetry and non-linearity properties. The knowledge gained may lead to a better understanding of the equation, and may also be useful in obtaining more accurate solutions. Let us define a transformation T_1 that does the following: $Z\to 1/Z$, $g_1 \longleftrightarrow -g_2$ and $g_3 \longleftrightarrow g_4$. It is easy to see that under this transformation, eq. (22) remains form-invariant. Thus, T_1 is a symmetry transformation. There is yet one more transformation T_2, say, which does the following. $Z\to 1/Z$, $g_1 \longleftrightarrow g_2$, $g_3 \longleftrightarrow -g_4$. T_2 is also a symmetry transformation. Let us define a new dependent variable

$$\eta = \frac{g_1 Z - g_2}{g_3 Z - g_4}. \tag{23}$$

It is easily seen that

$$T_i\,\eta = -\,\eta;\quad i = 1, 2. \tag{24}$$

These considerations help us to reduce the differential eq (22) to the following canonical form

$$\frac{d\eta}{dV} = a(V) + \eta b(V) + \eta^2 c(V) + \eta^3 d(V) \tag{25}$$

where a, b, c, d are known functions of $g_i(V)$ and their first derivatives. We note that we do not have to use any specific properties of g_i to come so far, except that the locations of the singularities of a, b, c, d will depend upon the actual forms of the g_i. At the positions of these singularities the above considerations will not hold. Bearing this precaution in mind, we may claim that any differential equation of the form of eq. (22), with arbitrary g_i, can always be reduced to the canonical form eq. (25). The latter may be compared with another nonlinear equation, namely, the Riccati equation which has terms up to the quadratic in the dependent variable on the right hand side. Thus, eq. (25) proves to be even more non-linear than the Riccati equation. In general, the Riccati equation cannot always be solved. However, if one solution is known, another can always be constructed from it. Whether such is also the case for eq. (25) remains to be investigated. However, eq. (25) must have at least two distinct solutions; one corresponding to the imploding motion and another corresponding to the exploding motion of the shock-front.

3. Formal exact solution

If we let $q = g_3 Z - g_4$, we can reduce eq. (22) to the following form

$$\frac{dq}{dV} - P(V)q - Q(V) = \frac{R(V)}{q} \tag{26a}$$

where P, Q, R are known functions of the g_i and their first derivatives:

$$P = (g_3' + g_1)/g_3; \quad Q = (g_4 g_3' + 2g_1 g_4 - g_2 g_3 - g_4' g_3)/g_3$$
$$R = (g_1 g_4^2 - g_2 g_3 g_4)/g_3. \tag{26b}$$

Here prime denotes differentiation with respect to V. The left hand side of eq. (26) has the standard form of a linear differential equation. However, we must show that the right hand side is well defined at $q = 0$, before we can utilize this interesting connection with the linear differential equation. We proceed as follows. The physical quantities u, ρ, c must remain finite for finite values of r. Therefore, from eqs (11), (15) and (17), it is clear that as $s \to 0$,

$$V(s) \to s \tag{27}$$

$$Z(s) \to s^2 \tag{28}$$

or (Zeldovich and Raizer 1967).

$$Z(V) \to V^2; \quad \text{as } V \to 0. \tag{29}$$

Now $g_4 \to V$ and $g_3 \to$ constant, as $V \to 0$. Therefore, $q \to 0$ in the same limit. However, $R(V)$ is such that $R(V)/q$ goes to a finite limit, as $V \to 0$. Thus eq. (26) remains well defined at $q = 0$. This enables us to write a formal solution of eq. (26) in terms of recurring continued fractions as follows:

$$q = A(V) + E(V) \int^{V} \frac{R(V)\, dV}{A(V) + E(V) \int \frac{R(V)\, dV}{A(V) + \ldots}} \tag{30}$$

where

$$q = g_3 Z - g_4 \tag{31}$$

$$A(V) = E(V) \int \frac{Q(V)\, dV}{E(V)} \tag{32}$$

$$E(V) = \exp\left(\int P(V) dV\right). \tag{33}$$

Having solved for $Z = Z(V)$, one can use eq. (19) to solve for $s = s(V)$ by a mere quadrature. The adiabatic integral provides the third exact solution. Thus we have, in principle, a complete set of exact solutions. However, they are not very useful in practice, because of the integrations over continued fractions involved in eq. (30). Therefore, we turn to approximate solutions.

4. Approximate solutions

4.1. *Initial boundary conditions*

To determine the initial boundary conditions for the three types of shocks, namely, the $1S$, the $1S(m-1)W$ and the mW cases, we proceed as follows. Let us consider an infinitesimally thin surface of discontinuity moving with a radial velocity D_1 from region 1 towards region 0 which is closer to the centre of symmetry. In the rest frame of the surface of discontinuity the integration of eqs (1)–(3) leads to the following jump conditions:

$$(u_1 - D_1)\, \rho_1 = (u_0 - D_1)\, \rho_0 \tag{34}$$

$$p_1 + \rho_1 (u_1 - D_1)^2 = p_0 + \rho_0 (u_0 - D_1)^2 \tag{35}$$

$$\epsilon_1 + \tfrac{1}{2}(u_1 - D_1)^2 + p_1/\rho_1 = \epsilon_0 + \tfrac{1}{2}(u_0 - D_1)^2 + p_0/\rho_0 \tag{36}$$

where ϵ is the internal energy per unit mass. Assuming the isentropic equation of state for an ideal gas, one can show that (Jha and Chavda 1977) the jump conditions for a single strong shock ($p_1/p_0 \gg 1$) reduce to

$$\rho_1/\rho_0 \simeq (\gamma + 1)/(\gamma - 1) \tag{37a}$$

$$u_1 \simeq -\frac{c_0}{\gamma}\left(\frac{2\gamma}{\gamma + 1}\right)^{1/2} (p_1/p_0)^{1/2} \tag{37b}$$

$$D_1 \simeq -c_0 \left(\frac{\gamma + 1}{2\gamma}\right)^{1/2} (p_1/p_0)^{1/2} \tag{37c}$$

where u_0, the gas speed in the undisturbed gas, is taken to be zero. In terms of the reduced functions these boundary conditions for the $1S$ case are

$$V(s = -1) \simeq 2\alpha/(\gamma+1) \tag{38a}$$

$$Z(s = -1) \simeq 2\gamma(\gamma-1)\alpha^2/(\gamma+1)^2 \tag{38b}$$

$$G(s = -1) \simeq (\gamma+1)/(\gamma-1). \tag{38c}$$

To get the jump conditions for the mW case, one must iterate eqs (34–36). On doing so, one gets (Jha and Chavda 1977)

$$\rho_m/\rho_0 \simeq (p_m/p_0)^{1/\gamma} \tag{39a}$$

$$u_m \simeq -\frac{2c_0}{\gamma+1}(p_m/p_0)^{(\gamma-1)2/\gamma} \tag{39b}$$

$$D_m \simeq -c_0\left(\frac{\gamma+1}{\gamma-1}\right)(p_m/p_0)^{(\gamma-1)/2\gamma}. \tag{39c}$$

Here we have used the notation in which the quantities in the region between shocks n and $n+1$, are labelled by n and we have assumed that $p_n/p_{n-1} - 1 \ll 1$, $m \geqslant n \geqslant 1$, and $(p_m/p_0)^{(\gamma-1)/2\gamma} \gg 1$. In terms of the reduced functions, for the boundary values in the mW case one gets

$$V(-1) \simeq 2\alpha/(\gamma+1) \tag{40a}$$

$$Z(-1) \simeq \alpha^2(\gamma-1)^2/(\gamma+1)^2 \tag{40b}$$

$$G(-1) \simeq (p_m/p_0)^{1/\gamma} \tag{40c}$$

where $V(-1)$ refers to the value of $V(s)$ at $s = -1$. Similarly for the $1S(m-1)W$ case one gets

$$\rho_m/\rho_0 \simeq \left(\frac{\gamma+1}{\gamma-1}\right)(p_m/p_1)^{1/\gamma} \tag{41a}$$

$$u_m \simeq -\frac{2c_1}{\gamma-1}(p_m/p_1)^{(\gamma-1)/2\gamma} \tag{41b}$$

$$D_m \simeq -c_1\left(\frac{\gamma+1}{\gamma-1}\right)(p_m/p_1)^{(\gamma-1)/2\gamma} \tag{41c}$$

where $(p_m/p_1)^{(\gamma-1)/2\gamma} \gg 1$ and $p_1/p_0 \gg 1$, but $(p_n/p_{n-1}) - 1 \ll 1$, for $m \geqslant n \geqslant 2$. Thus, for the $1S\,(m-1)W$ case, one gets the boundary conditions:

$$V(-1) \simeq 2\alpha/(\gamma+1) \tag{42a}$$

$$Z(-1) \simeq \alpha^2(\gamma-1)^2/(\gamma+1)^2 \tag{42b}$$

$$G(-1) \simeq \left(\frac{\gamma+1}{\gamma-1}\right)(p_m/p_1)^{1/\gamma} \tag{42c}$$

4.2. *Determination of the self-similarity index* α

The solutions in the region A are the trivial undisturbed ones. In the region B, the $Z-V$ curve must pass through the origin 0 as is clear from eq. (29). This is true

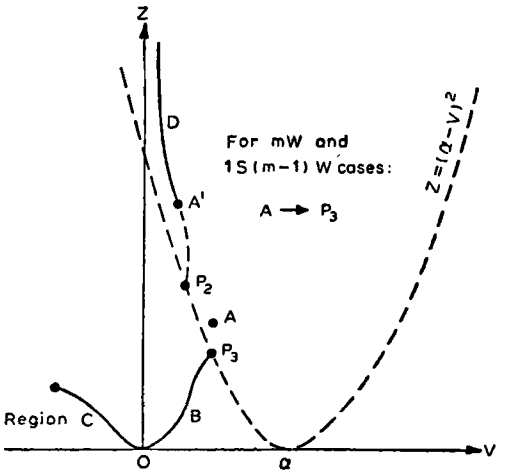

Figure 1. Possible physical integral curves in different regions of the V—Z plane, and the location of singular points (P_2, P_3), and the initial boundary points (A, A'). Only the solid curves represent possible solutions for the mW and the $1S(m-1)W$ cases. For the $1S$ case the physical curve has to extend up to the point A given by $[2\alpha/(\gamma+1),\ 2\gamma(\gamma-1)\alpha^2/(\gamma+1)^3]$.

for all three cases under consideration. Another point which the $Z-V$ curve in the region B must pass through is the boundary point $s=-1$. We denote it as A in figure 1. Its coordinates are given by eqs (38), (40) and (42) for the three cases under consideration. For the $1S$ case, it lies above the parabola $\triangle=(\alpha-V)^2-Z=0$. For the other two cases it lies almost on the parabola; albeit slightly above it. Thus, in all three cases, the $Z-V$ curve must pass through points 0 and A which lie on the opposite sides of the parabola $\triangle=0$ (see figure 1). Therefore the curve must intersect the parabola. The points of intersection will, in general, be extrema of the $s=s(V)$ curve as is evident from eq. (19). The single valuedness of the physical quantities requires that there be no extrema at the points of intersection. This can only be achieved by demanding that $\triangle_1$ also vanish when $\triangle=0$. This determines the singular points of the differential equation (19) as

$$V_{\pm}=B_{\pm}\,(B^2-\mu\,\alpha/N)^{1/2} \tag{43}$$

and

$$Z_{\pm}=(\alpha-V_{\pm})^2 \tag{44}$$

where

$$B=(\mu+(N+1)\,\alpha-1)/2N;\ \mu=2(1-\alpha)/\gamma. \tag{45}$$

Let us denote by P_3 and P_2 the points obtained by taking the upper and the lower signs, respectively, in eqs (43) and (44). The imploding (exploding) solution must pass through the point $P_3(P_2)$ as shown in figure 1.

Since the point A lies almost on the parabola for the mW and the $1S\,(m-1)W$

cases, we equate the abscissa of A given by eqs (40a) and (42a) with the abscissa V_+ of P_3 given by eq. (43). This immediately determines the similarity index α as

$$\alpha = \frac{(\gamma+1)(2\gamma-1)}{(N+2)\gamma^2-(N-1)\gamma-1}. \tag{46}$$

For the spherical ($N = 2$) and the cylindrical ($N = 1$) geometries the values of α are $14/19 = 0{\cdot}736842$ and $\alpha = 28/33 = 0{\cdot}848485$, respectively, when $\gamma = 5/3$. These considerations do not apply to the $1S$ case, since there the boundary point A is distinct from the point P_3. For the latter one has to find a solution that passes through the origin and has a constant of integration. The solution must also pass through the distinct points A and P_3. This leads to over-determination of the solution, i.e., a relation between α and γ. For a given approximate solution one can explicitly display this relationship between α and γ. For the $1S$ case, using the solutions presented in the next section, we get $\alpha = 0{\cdot}815567$ and $\alpha = 0{\cdot}688273$, for $N = 1$ and $N = 2$, respectively. For a more accurate value of α for the $1S$ case, one must solve the differential equation numerically (Zeldovich and Raizer 1967). Here, too, it is the over-determination of the solution that gives the value of α.

4.3. *Approximate solutions in regions B and C*

Using eq. (29), one can show that a quantity defined as

$$F(Z,V) = \frac{\triangle}{\triangle_1}\frac{V(V-1)}{(\alpha-V)} \tag{47}$$

tends to unity as $V \to 0$. Similarly, if the point P_3 is approached in such a way that $Z = Z_+ + \epsilon$, where ϵ approaches zero through positive values, and $V = V_+$, held fixed, F again tends to unity. Here V_+ and Z_+ are the coordinates of P_3 defined in eqs (43) and (44). However, for more general directions of approaching P_3 the quantity F may differ somewhat from unity at P_3. Let us see how to determine F at the point P_3, in the general case. From eqs (29) and (47) we may write F as

$$F = \frac{V(1-V)}{(N+1)\,[V-\mu/(N+1)]\,(\alpha-V)}\,\frac{Z-(\alpha-V)^2}{\left\{Z-\dfrac{V(1-V)\,(\alpha-V)}{(N+1)\,[V-\mu/(N+1)]}\right\}} \tag{48}$$

Now at P_3, $\triangle = \triangle_1 = 0$. That is,

$$(N+1)\left(V_+ - \frac{\mu}{N+1}\right)(\alpha-V_+) = V_+(1-V_+);\ \mu \equiv \frac{2(1-\alpha)}{\gamma}. \tag{49}$$

Using this, we have, at P_3

$$F = \lim_{\substack{V\to V_+\\ Z\to Z_+}} \frac{Z-(\alpha-V)^2}{Z-\dfrac{V(1-V)\,(\alpha-V)}{(N+1)\,[V-\mu/(N+1)]}}$$

$$= \frac{X_+ + C}{X_+ + D};\ X_+ \equiv \left(\frac{dZ}{dV}\right)_+ \tag{50}$$

where

$$C = 2(\alpha - V_+) \tag{51}$$

and

$$D = \frac{V_+(1-V_+)(\alpha-V_+)}{(N+1)\left(V_+ - \frac{\mu}{N+1}\right)^2} + \frac{V_+(1-V_+)}{(N+1)\left(V_+ - \frac{\mu}{N+1}\right)}$$

$$+ \frac{V_+(\alpha-V_+)}{(N+1)\left(V_+ - \frac{\mu}{N+1}\right)} - \frac{(1-V_+)(\alpha-V_+)}{(N+1)\left(V_+ - \frac{\mu}{N+1}\right)}. \tag{52}$$

We determine X_+ as follows. From eqs (18) and (19), we have

$$\frac{dZ}{dV} = Z\left[\frac{\gamma-1}{\alpha-V} - \frac{[1+(N+1)\gamma-2]V-2}{(N+1)(\alpha-V)\left[V - \frac{\mu}{N+1}\right]}\right.$$

$$\left. \times \frac{[Z-(\alpha-V)^2]}{\left[Z - \frac{V(1-V)(\alpha-V)}{(N+1)\left(V - \frac{\mu}{N+1}\right)}\right]}\right] \tag{53}$$

Hence,

$$X_+ - A_3 - B_3\left[\frac{X_+ + C}{X_+ + D}\right] \tag{54}$$

where, $A_3 = (\gamma-1)(\alpha-V_+)$

$$B_3 = \frac{[1+(N+1)\gamma-2]V_+-2}{(N+1)\left(V_+ - \frac{\mu}{N+1}\right)}. \tag{55}$$

For the mW and the $1S(m-1)W$ cases, with $N = 2$, we have

$$A_3 = \frac{7}{57}; \quad B_3 = \frac{28}{968}; \quad C = \frac{7}{19}; \quad D = \frac{14}{51}. \tag{56}$$

Using these values we can solve the quadratic eq. (54) to yield

$$X_{+-} = 0{\cdot}087; \quad X_{++} = -0{\cdot}266 \tag{57}$$

We expect the slope at P_3 to be positive. Therefore, using the first value X_{+-} in place of X_+ in eq. (50), we find

$$F = 1{\cdot}26 \text{ at } P_3. \tag{58}$$

Thus, even in the most general case, the value of F is close to unity at P_3. Keeping aside the problem of more accurate curve fitting for the future, we shall, therefore, make the simplest possible approximation here that $F \simeq 1$ throughout the region B. That is,

$$\frac{\triangle}{\triangle_1} \simeq \frac{(\alpha - V)}{V(V-1)}, \text{ everywhere in B.} \tag{59}$$

This approximation makes the right hand sides of eqs (18) and (19), functions of V only. Simple integration of these equations leads to the following approximate solutions.

$$Z \simeq |K_1| \frac{V^2 (1-V)^{(\gamma-1)(N+1)}}{(\alpha - V)^{\gamma-1}} \tag{60a}$$

$$s \simeq -|K_2| V(1-V)^{(1-\alpha)/\alpha} \tag{60b}$$

$$G \simeq |K_3| \frac{(1-V)^{N+1}}{(\alpha - V)} \tag{60c}$$

where the constants K_i can be determined from the initial boundary conditions (38), (40) and (42), for the three cases under consideration. Considering the boundary conditions, we find that in the region B

$$0 \leqslant V \leqslant \frac{2\alpha}{\gamma+1}, \text{ for all three cases.} \tag{61}$$

Our approximation (59) seems to be bad for the case of the $1S$ only, when we substitute the analytical solutions back into eq. (47). For other cases, our solutions are excellent.

In the region C, the quantities p, u, ρ, c will continue to develop as they did in the region B, because the reflected shock front has not yet arrived at the point of observation where these quantities are measured. Thus, we may analytically continue the approximate solutions, eqs (60), from the region B to the region C merely by changing s to $-s$. Having obtained the solutions in the region C, we now turn to calculate the important parameter, s^*, defined after eq. (14). This is obtained from (Jha and Chavda 1977)

$$1/s^* = 1 + \lim_{s \to 0} \left[\frac{V(s)}{\alpha s}\right] = 1 - \frac{2}{\gamma+1} \left[1 - \frac{2\alpha}{\gamma+1}\right]^{(1-\alpha)/\alpha}. \tag{62}$$

Since u and V are both negative in the region C, $s^* < 1$. Knowing s^*, and using the approximate solutions in the region C, we can calculate V, Z, G just before the reflected shock front reaches the point of observation. Let us denote these values by $V_c(s^*)$ $Z_c(s^*)$ and $G_c(s^*)$. These and the values of α and s^* are presented below for the three, cases under consideration when $\gamma = 5/3$. A comparison of eqs (40a), (40b), with eqs (42a), (42b) shows that the initial boundary conditions for the $Z = Z(V)$ curve for the mW and the $1S(m-1)W$ cases are the same. Then from eqs (60) it follows

that the constants K_1 and K_2 as also the parameters α and s^* are also the same for the two cases (Chavda 1977). Hence for the spherical geometry with $N=2$ we get the following common values for the two cases

$$\alpha \simeq 14/19 = 0{\cdot}736842 \tag{63a}$$

$$s^* \simeq 2{\cdot}29 \tag{63b}$$

$$V_c(s^*) \simeq 0{\cdot}77 \tag{63c}$$

$$Z_c(s^*) \simeq 0{\cdot}26. \tag{63d}$$

However, the values $G_c(s^*)$ are different for the two cases and are given by

$$G_c(s^*) \simeq 30{\cdot}4 \left(\frac{\gamma-1}{\gamma+1}\right)(p_m/p_0)^{1/\gamma} \text{ for } mW \tag{63e}$$

$$G_c(s^*) \simeq 121{\cdot}6 \left(\frac{\gamma-1}{\gamma+1}\right)(p_m/p_1)^{1/\gamma} \text{ for } 1S(m-1)W. \tag{63f}$$

For the cylindrical geometry, with $N=1$, we have the following common values for the mW and the $1S(m-1)W$ cases

$$\alpha \simeq 28/33 = 0{\cdot}848485 \tag{64a}$$

$$s^* \simeq 2{\cdot}67 \tag{64b}$$

$$V_c(s^*) \simeq -1{\cdot}23 \tag{64c}$$

$$Z_c(s^*) \simeq 0{\cdot}41 \tag{64d}$$

and

$$G_c(s^*) \simeq 15{\cdot}36 \left(\frac{\gamma-1}{\gamma+1}\right)(p_m/p_0)^{1/\gamma} \text{ for } mW \tag{64e}$$

$$G_c(s^*) \simeq 61{\cdot}44 \left(\frac{\gamma-1}{\gamma+1}\right)(p_m/p_1)^{1/\gamma} \text{ for } 1S(m-1)W. \tag{64f}$$

As already stated, the approximate solutions, eq. (60), are not appropriate for the $1S$ case because the values of various parameters, except that of α, calculated therefrom deviate substantially from the exact ones, known from previous numerical work (Goldman 1977). We will not consider the $1S$ case any more in the context of our present approximation scheme in the regions B and C.

4.4. *Exact asymptotic solution in the region D*

At $s=s^*$ the various quantities undergo further shock discontinuities given by (Jha and Chavda 1977)

$$V_D = V_c + \left(\frac{2}{\gamma+1}\right)\frac{Z_c-(\alpha-V_c)^2}{(V_c-\alpha)} \tag{65a}$$

$$G_D = G_c\left[\frac{V_c-a}{V_D-a}\right] \tag{65b}$$

$$Z_D = \left(\frac{\gamma-1}{\gamma+1}\right)^2\left[1+\left(\frac{2}{\gamma-1}\right)\frac{Z_c}{(a-V_c)^2}\right]\left[\left(\frac{2\gamma}{\gamma-1}\right)(V_c-a)^2-Z_c\right] \tag{65c}$$

where $V_c = V_c(s^*)$, $V_D = V_D(s^*)$, etc. Equation (65) provides the starting values for the integral curves in the region D. The motion in the region D is again self-similar with the same a. However, the solution must now be of the explosive type, i.e., $-a\,d\ln|s|/dV<0$. It must also pass through the singular point P_2 of figure 1.

In the following, we present, for the first time, the exact asymptotic solution in the region D. We also give solutions that serve as good approximations throughout the region D. In the asymptotic region, $Z\to\infty$ and $s\to\infty$. It is clear from eq. (19) that unless

$$V\to V_\infty = \mu(N-1);\ \mu = \frac{2(1-a)}{\gamma} \tag{66}$$

and

$$Z\to\frac{C}{V-V_\infty},\ \text{as } s\to\infty \text{ and } Z\to\infty \tag{67}$$

with

$$C<\lambda_2 \tag{68}$$

where

$$\lambda_2 = \frac{V_\infty}{N+1}(1-V_\infty)(a-V_\infty) \tag{69}$$

the solution will not be of the explosive type. The constant C is determined by a self-consistency condition, viz., that the logarithmic derivative of Z, obtained from eq. (67), must equal that obtained from eq. (18), in the asymptotic region. This determines C uniquely as

$$C = \lambda_2/(1+\lambda_1) \tag{70}$$

where

$$\lambda_1 = \frac{2-V_\infty[(N+1)\gamma-N+1]}{(N+1)(a-V_\infty)} \equiv \frac{d_1}{(N+1)(a-V_\infty)}. \tag{71}$$

For both the mW and the $1S(m-1)W$ cases we have $C=0{\cdot}015$ and $C=0{\cdot}01082$ for $N=1$ and $N=2$ respectively. For the $1S$ case the corresponding values are $C=0{\cdot}016$ and $C=0{\cdot}01086$, respectively, This implies that, asymptotically, the reduced sound velocity $\sqrt{Z}$ is higher for the $1S$ case than for the other two cases, for both geometries. Equation (67) with parameters given by eqs (70) and (71) gives the exact asymptotic

solutions. A nontrivial asset of eq. (67) is that it has no free parameters. The condition, eq. (68), for the asymptotic solution to be of the explosive type reduces to

$$\alpha/(1-\alpha)>(1-N)/[\gamma(1+N)]. \tag{72}$$

For the cylindrical ($N=1$) and the spherical ($N=2$) geometries, this condition is trivially satisfied, thus ensuring that our asymptotic solution is indeed of the explosive type. The remaining asymptotic solutions can be obtained as follows. Substituting eq. (68) into eq. (19) gives

$$s=k_s(V-V_\infty)^{-p_s} \text{ as } s\to\infty,\ V\to V_\infty \tag{73}$$

with

$$1/p_s = \alpha(N+1)\lambda_1. \tag{74}$$

Substituting eq. (73) into eq. (18), we find a solution that not only goes over to eq. (67) in the asymptotic region, but also serves as a fairly good approximation in the whole of the D region. It is

$$Z=k_Z(\alpha-V)^{-q_1}/(V-V_\infty) \tag{75}$$

where

$$k_Z=Z_D(\alpha-V_D)^{q_1}(V_D-V_\infty) \tag{76}$$

and

$$q_1=\gamma-1+[(1+(N+1)\gamma-N)\alpha-2]/d_1 \tag{77}$$

and where V_D, Z_D, etc. are defined by eq. (65) and d_1 is defined by eq. (71). Substitution of eqs (73) and (75) into the adiabatic integral, eq. (20), leads to

$$\bar{G}=\bar{k}_g(\alpha-V)^{-b_1}(V-V_\infty)^{b_2} \tag{78}$$

where

$$\bar{G}=(\rho/\rho_0)\left(\frac{\gamma+1}{\gamma-1}\right)(p_m/p_l)^{-1/\gamma} \tag{79}$$

$$b_1=1+\alpha\,(N+1)/d_1 \tag{80}$$

$$b_2=\mu/d_1. \tag{81}$$

In eq. (79), $p_l=p_0$ for the mW case and $p_l=p_1$ for the $1S(m-1)W$ case. The constant $\bar{k}_g$ in eq. (78) is determined from

$$\bar{k}_g = \bar{G}_D(\alpha-V_D)^{b_1}/(V_D-V_\infty)^{b_2}. \tag{82}$$

Using eqs (63), (64) and (65), we get the following common starting values for the mW and the $1S(m-1)W$ cases for the spherical geometry, $N=2$:

$$V_D(s^*)\simeq 0{\cdot}23 \tag{83a}$$

$$Z_D(s^*)\simeq 0{\cdot}93 \tag{83b}$$

and

$$G_D(s^*) \simeq 90{\cdot}84\left(\frac{\gamma-1}{\gamma+1}\right)(p_m/p_0)^{1/\gamma} \text{ for } mW \tag{83c}$$

$$G_D(s^*) \simeq 363{\cdot}36\left(\frac{\gamma-1}{\gamma+1}\right)(p_m/p_1)^{1/\gamma} \text{ for } 1S(m-1)W. \tag{83d}$$

Similarly the common starting values for the two cases for the cylindrical geometry, $N=1$, are:

$$V_D(s^*) \simeq 0{\cdot}18 \tag{84a}$$

$$Z_D(s^*) \simeq 1{\cdot}70 \tag{84b}$$

and

$$G_D(s^*) \simeq 47{\cdot}76\left(\frac{\gamma-1}{\gamma+1}\right)(p^m/p_0)^{1/\gamma} \text{ for } mW \tag{84c}$$

$$G_D(s^*) \simeq 191{\cdot}04\left(\frac{\gamma-1}{\gamma+1}\right)(p_m/p_1)^{1/\gamma} \text{ for } 1S(m-1)W \tag{84d}$$

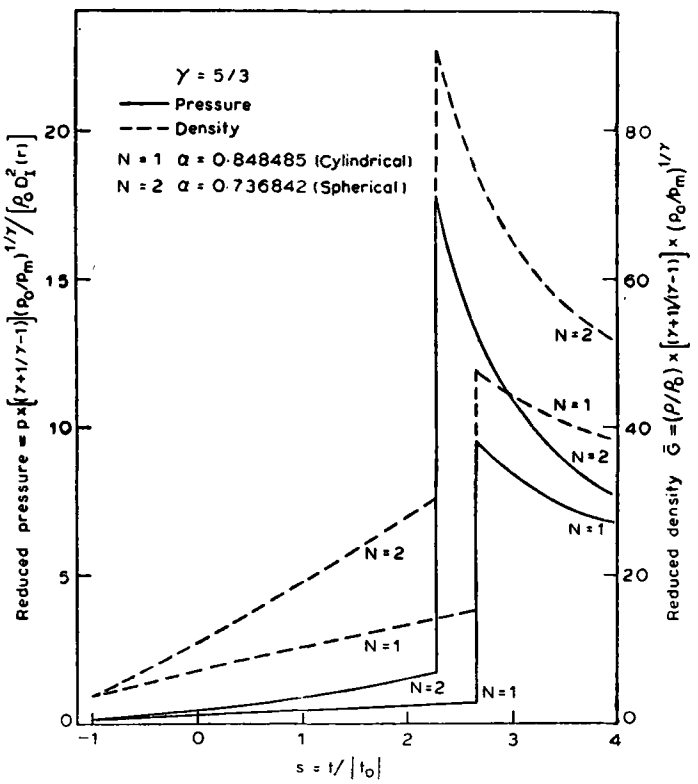

Figure 2. Plots of reduced pressure (left scale) and reduced mass density (right scale) as functions of $s=t/|t_0|$. Curves are presented for the mW case only. The curves with $N=1$ and $N=2$ refer to the cylindrical and the spherical geometries, respectively. Curves for the $1S(m-1)W$ case may be obtained by multiplying all ordinates by a factor 4, and by replacing p_0 by p_1.

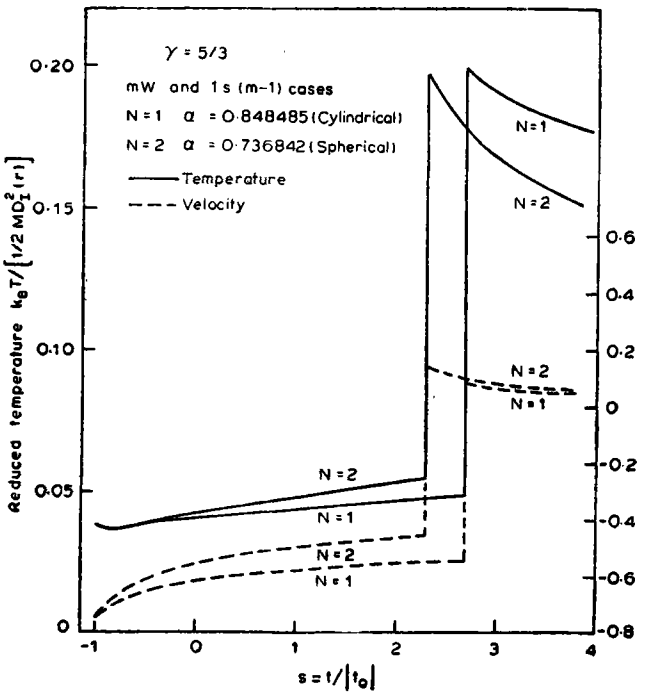

Figure 3. Plots of reduced temperature (left scale) and reduced fluid velocity (right scale) as functions of s. The reduced temperature and the reduced fluid velocity are the same for the mW and the $1S(m-1)W$ cases. The labels $N=1$ and $N=2$ refer to the cylindrical and the spherical geometries respectively.

In figures 2 and 3 we plot the following reduced quantities:

$$u/|D_I(r)| = V/(\alpha s) \tag{85a}$$

$$\left[p\Big/\left(\rho_0 D_I^2(r)\right)\right]\left(\frac{\gamma+1}{\gamma-1}\right)(p_i/p_m)^{1/\gamma} = Z\bar{G}/(\gamma\alpha^2 s^2) \tag{85b}$$

$$k_B T/(\tfrac{1}{2}MD_I^2(r)) = Z/(\gamma\alpha^2 s^2) \tag{85c}$$

where k_B is the Boltzmann constant and T is the absolute temperature, and $p_i = p_0$ for the mW case and $p_i = p_1$ for the $1S(m-1)W$ case. From figures 2 and 3 we see that the reduced pressure, eq. (85b), the reduced density, eq. (79), and the reduced fluid velocity, eq. (85a), are always higher for spherical geometry than for the cylindrical geometry. This, however, is not true for the reduced temperature,eq. (85c). From figure 3, we see that although the reduced temperatures in the spherical geometry are higher than those in the cylindrical geometry for the imploding shocks, the situation is reversed for the reflected shocks. In fact, from eq. (85c) and figure 3, it is clear that the choice of the geometry depends upon the relative values of two parameters, namely, $D_I(r)$ and $|t_0|$. The former is the speed of the incident shock front when it reaches the point of observation, and the latter is the time taken by the incident shock to travel from the point of observation to $r=0$. In particular, if these values are the same for the two geometries, then the cylindrical geometry is preferable

to the spherical one as it (the former) not only gives higher final absolute temperatures it also yields lower initial temperatures; a most desirable combination to have, for thermonuclear fusion in *DT* plasmas.

5. Discussion

In this paper we have presented approximate but sufficiently accurate solutions for implosion in spherical and cylindrical geometries. In the regions B and C, these simple approximate solutions work very well for the mW and the $1S(m-1)W$ cases but not so well for the $1S$ case. In order to get good results for the $1S$ case, and more accurate results for the mW and $1S(m-1)W$ cases, in the regions B and C, we will have to fitthe function $F(Z, V)$ of eq. (47) by a higher order polynomial in V, the coefficients of which have to be determined self-consistently, using the boundary values and the differential eq. (53). Here, we have made the lowest order polynomial approximation, by taking $F=1$, everywhere in the regions B and C. However, the extension of our approximation scheme to higher-order poylnomials, as successive approximations, is quite clear. We hope to take up this problem in the near future, to obtain results converging to the exact situation. We have also presented, for the first time, the exact asymptotic solutions, in the region D, in analytic form, for the reflected shocks. These solutions are applicable to all the three types of shocks mentioned above. In particular, the solution for the reduced sound speed, $Z^{1/2}$, eq. (67), has no free parameters and predicts that, asymptotically, the reduced sound speed is always higher for the $1S$ case than for the other two cases in the spherical as well as the cylindrical geometries. We have also presented solutions that serve as good approximations throughout the region D. Criteria for making the choice between the two geometries are also given. As we have neglected self-heating, our solutions in the region D will remain valid up to the point before the absorption of α particles generated in thermonuclear D-T reactions becomes appreciable, after the shock reflection.

Acknowledgement

One of us (LKC) thanks the Theoretical Physics Division of TIFR, for hospitality during the summer of 1977, when a major part of this work was completed.

References

Bogolyubskii S L *et al* 1976 *JETP Lett.* **24** 183
Chang J, Widner M M, Kuswa G W and Yonas G 1975 *Phys. Rev. Lett.* **34** 1266
Chavda L K 1977 to be published in *Phys. Lett.* A
Clauser M J *et al* 1977 *Phys. Rev. Lett.* **38** 398
Goldman E B 1977 *Plasma Phys.* **15** 289
Guderley G 1942 *Luftfahrtforschung* **19** 302
Jha S S and Chavda L K 1977 *Phys. Rev.* **A15** 1289
Stanyukovich K P 1960 *Unsteady Motions of Continuous Media* (London: Pergamon) Sec. 64
Zeldovich Y B and Raizer Y P 1967 *Physics of the Shock Waves and High Temperature Hydrodynamic Phenomena* Vols I and II (New York: Academic Press) Ch. 12